Chemical Science

ROYAL SOCIETY OF CHEMISTRY

EDGE ARTICLE

View Article Online
View Journal | View Issue

Cite this: *Chem. Sci.*, 2022, **13**, 8576

All publication charges for this article have been paid for by the Royal Society of Chemistry

Received 16th May 2022
Accepted 21st June 2022

DOI: 10.1039/d2sc02721f

rsc.li/chemical-science

Nickel^{II}-catalyzed asymmetric photoenolization/Mannich reaction of (2-alkylphenyl) ketones†

Liangkun Yang, Wang-Yuren Li, Liuzhen Hou, Tangyu Zhan, Weidi Cao,* Xiaohua Liu and Xiaoming Feng *

A diastereo- and enantioselective photoenolization/Mannich (PEM) reaction of *ortho*-alkyl aromatic ketones with benzosulfonimides was established by utilizing a chiral *N*,*N*′-dioxide/Ni(OTf)$_2$ complex as the Lewis acid catalyst. It afforded a series of benzosulfonamides and the corresponding ring-closure products, and a reversal of diastereoselectivity was observed through epimerization of the benzosulfonamide products under continuous irradiation. On the basis of the control experiments, the role of the additive LiNTf$_2$ in achieving high stereoselectivity was elucidated. This PEM reaction was proposed to undergo a direct nucleophilic addition mechanism rather than a hetero-Diels–Alder/ring-opening sequence. A possible transition state model with a photoenolization process was proposed to explain the origin of the high level of stereoinduction.

Introduction

Photoinduced catalysis contributes in a significant way to the existing repertoire of carbon–carbon and carbon-hetero bond-forming reactions,[1] allowing exceptional molecular transformations complementary to thermal catalytic reactions.[2] Aromatic aldehydes and ketones represent an important subset of carbonyl compounds, which can undergo unique reaction pathways upon irradiation with UV light.[3] As a kind of classic Norrish type II process, the photoenolization of 2-alkylphenyl containing carbonyls has been thoroughly studied since 1961.[4] Therein, the photogenerated enols possess fascinating reactivities and have been regarded as versatile intermediates in diverse reactions.[5] Nevertheless, the enantioselective versions were relatively limited. Early attempts focused on the asymmetric photoenolization/Diels–Alder (PEDA) reactions; Bach[6] and Nicolaou[7] obtained considerable results with the use of a stoichiometric catalyst. Later, Melchiorre creatively realized the enantioselective PEDA reaction with maleimides by using a cinchona-thiourea catalyst,[8] and Gao's group took the PEDA reaction as a key step catalyzed by Ti–TADDOL complexes in asymmetric synthesis of natural products.[9] In addition to dienophiles, other reaction partners to trap the ephemeral photoenols enantioselectively have been exploited, such as in the Michael reaction[10] and aldol[11] and allylic alkylation-type reactions.[12] By contrast, the catalytic asymmetric photoenolization/Mannich reaction (PEM) seemed to encounter challenges such as: (1) the irrepressible background reaction and (2) the potential epimerization of the product due to its further photoenolization. Melchiorre first disclosed the enantioselective PEM reaction with *N*-protected benzaldimines promoted by a chiral (DHQ)$_2$PHAL catalyst, affording the desired chiral amines with moderate enantioselectivity and low diastereoselectivity (Scheme 1a).[13] Recently, He's group realized

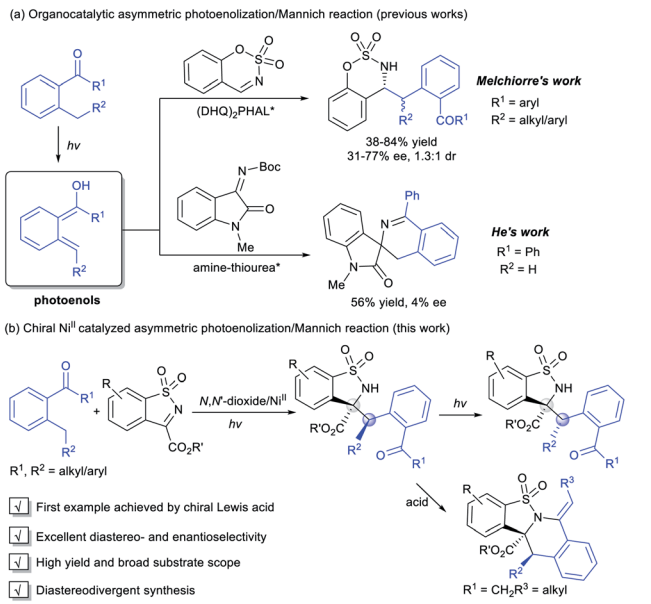

Scheme 1 The catalytic asymmetric PEM reactions of 2-alkylphenyl ketones.

Key Laboratory of Green Chemistry & Technology, Ministry of Education, College of Chemistry, Sichuan University, Chengdu 610064, China. E-mail: wdcao@scu.edu.cn; xmfeng@scu.edu.cn

† Electronic supplementary information (ESI) available: ^{1}H, ^{13}C{^{1}H} and ^{19}F{^{1}H} NMR, HPLC spectra, and CD spectra. X-ray crystallographic data for **C1**, **E1** and **F1′**. CCDC 2081680, 2130299 and 2171982. For ESI and crystallographic data in CIF or other electronic format see https://doi.org/10.1039/d2sc02721f

an organocatalytic enantioselective aldol reaction of photoenol with isatin, but isatin-derived ketimine transformed into the spirocyclic oxindole in an uncontrolled manner (Scheme 1a).[11b]

Upon our long-term research, chiral *N*,*N*′-dioxide/metal complexes were demonstrated to exhibit excellent ability of chiral induction and delivery in asymmetric catalysis, including light-triggered reactions.[14] We conceived that this kind of powerful Lewis acid catalyst could activate imines to trap the photoenol intermediate and suppress the background reaction. Herein, we disclosed the first Ni^{II}-mediated highly diastereo- and enantioselective PEM reaction of acyclic and cyclic 2-alkylphenyl ketones with *N*-sulfonyl ketimines, delivering various optically active α-amino acetate derivatives under mild conditions. The adducts could further undergo ring-closure to produce the tetrahydroisoquinoline derivatives under acidic conditions in one pot. The epimers could be obtained with high enantioselectivity under continuous stronger irradiation (Scheme 1b).

Results and discussion

In our initial investigation, the *N*-sulfonyl cyclic ketimine **A1** and 2-benzylbenzophenone **B1** were applied as the model substrates to optimize the reaction conditions. The desired PEM reaction product **C1** was formed in a yield of 67% with 56 : 44 dr under 20 W UV LED irradiation in CH_2Cl_2, revealing the completion of a severe background reaction (Table 1, entry 1). To our delight, upon screening of metal salts (Table 1, entries 2–5) coordinated with chiral *N*,*N*′-dioxide **L_3-PiAd**, we found that $Ni(OTf)_2$ could provide promising enantioselectivity (68% yield, 58 : 42 dr, 57%/52% ee; entry 5). Other metal ions, such as Sc^{III}, Mg^{II}, and Zn^{II} yielded the product with no more than 5% ee. To improve the yield and stereoselectivity, additives and ligands were screened (see the ESI† for details). It was found that $LiNTf_2$ played a crucial role in promoting diastereo- and enantioselectivity, and **C1** could be isolated in 94% yield with 74 : 26 dr and 89%/85% ee by increasing its dosage to 30 mol% (Table 1, entry 6), which may benefit from exchanging the counterion with $Ni(OTf)_2$.[15] Switching the ligand from **L_3-PiAd** to **L_3-PiMe$_2$Br**, the ee value of the major diastereomer was slightly improved to 92% (Table 1, entry 7). Considering that the occurrence of epimerization of the product **C1** through the second photoenolization may provide the variation of diastereoselectivity, the intensity of the light source was reduced (entries 8 and 9). To our delight, a remarkable increase in diastereoselectivity was realized under 2 W UV LED irradiation albeit prolonged reaction time was necessary (8 h), and **C1** was obtained in 90% yield, 91 : 9 dr and 93% ee (Table 1, entry 9). Increasing the amount of **B1** and lowering the reaction concentration enhanced the yield to 96% with maintained stereoselectivity (entry 10). The exploration of wavelength showed that the reactivity reduced with the increase in the wavelength. Under the irradiation with a 385 nm UV LED, low diastereoselectivity (58 : 42) was obtained (entry 11). The PEM reaction could occur even with visible light (400 nm), but lower yield and stereoselectivity were obtained (entry 12). Other reaction parameters, including solvent, temperature and so on

Table 1 Optimization of the reaction conditions[a]

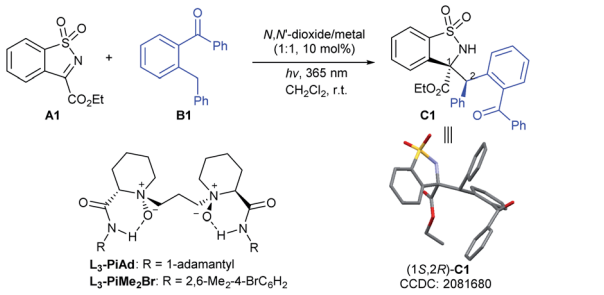

Entry	Metal salt	Ligand	Yield[b] (%)	dr[c]	ee[d] (%)
1	—	—	67	56 : 44	—
2	$Sc(OTf)_3$	**L_3-PiAd**	67	54 : 46	0
3	$Mg(OTf)_2$	**L_3-PiAd**	76	64 : 36	4/9
4	$Zn(OTf)_2$	**L_3-PiAd**	67	53 : 47	5/5
5	$Ni(OTf)_2$	**L_3-PiAd**	68	58 : 42	57/52
6[e]	$Ni(OTf)_2$	**L_3-PiAd**	94	74 : 26	89/85
7[e]	$Ni(OTf)_2$	**L_3-PiMe$_2$Br**	91	72 : 28	92/84
8[e,f]	$Ni(OTf)_2$	**L_3-PiMe$_2$Br**	89	85 : 15	93/76
9[e,g]	$Ni(OTf)_2$	**L_3-PiMe$_2$Br**	90	91 : 9	93/64
10[e,h]	$Ni(OTf)_2$	**L_3-PiMe$_2$Br**	96	92 : 8	93/65
11[e,h,i]	$Ni(OTf)_2$	**L_3-PiMe$_2$Br**	92	58 : 42	91/71
12[e,h,j]	$Ni(OTf)_2$	**L_3-PiMe$_2$Br**	87	90 : 10	91/52

[a] Unless otherwise noted, all reactions were carried out with $Ni(OTf)_2$/**ligand** (1 : 1, 10 mol%), **A1** (0.10 mmol), and **B1** (0.15 mmol) in CH_2Cl_2 (1.5 mL) at room temperature under a N_2 atmosphere and irradiation (20 W UV LED, λ_{max} = 365 nm) for 2.5 h. [b] Isolated yield. [c] The dr value was determined by ^{1}H NMR analysis. [d] Determined by UPC^2 on a chiral stationary phase. [e] With $LiNTf_2$ (30 mol%). [f] Under irradiation with a 5 W UV LED for 5 h. [g] Under irradiation with a 2 W UV LED for 8 h. [h] In CH_2Cl_2 (2.5 mL) and **B1** (0.2 mmol) were used. [i] Under irradiation with a 2 W UV LED (λ_{max} = 385 nm) for 8 h. [j] Under irradiation with a 2 W blue LED (λ_{max} = 400 nm) for 16 h.

were also examined, but no better result was obtained (see the ESI† for details). The absolute configuration of **C1** was determined to be (1*S*,2*R*) based on X-ray single crystal analysis.[16a]

With the optimized reaction conditions in hand, the substrate scope with respect to **A** was then evaluated (Table 2). Variations of the ester substituent of *N*-sulfonyl cyclic ketimines showed no obvious influence on the reactivities and stereoselectivities (Table 2, entries 1–4, 96–99% yields, 87 : 13–94 : 6 dr and 86–95% ee). Regardless of the position and electronic properties of the substituents on the phenyl ring, a wide range of substituted cyclic ketimines were converted into the corresponding products **C5–C13** with good to excellent yields (Table 2, entries 5–13, 80–93%). In general, the imines bearing electron-donating groups, such as **A5** (5-^{t}Bu), **A6** (5-OMe), **A9** (5,6-dimethoxy), and **A10** (6-Me), exhibited relatively low reactivity and required prolonged reaction time (8–56 h) with consistently good diastereo- and enantioselectivities (Table 2, entries 5–6, 9–10; 84 : 16–90 : 10 dr and 91–94% ee). When electron-deficient imines were used, the corresponding products (**C7**, **C8** and **C10–C13**) were obtained with decreased diastereo- and enantioselectivities, which may be attributed to the strong background reaction (Table 2, entries 7–8, 11–13,

Table 2 Substrate scope of *N*-sulfonyl cyclic ketimines

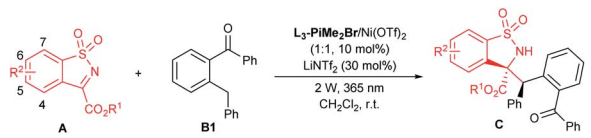

Entry[a]	R^1/R^2	t (h)	Yield[b] (%)	dr[c]	ee[d] (%)
1	Et/H	8	**C1**, 96	92 : 8	93
2	Me/H	8	**C2**, 98	87 : 13	86
3	^{i}Pr/H	8	**C3**, 99	94 : 6	95
4	Bn/H	8	**C4**, 99	88 : 12	88
5	Et/5-^{t}Bu	8	**C5**, 93	90 : 10	91
6	Et/5-OMe	32	**C6**, 80	84 : 16	93
7	Et/5-OCF_3	8	**C7**, 87	80 : 20	75
8	Et/5-F	8	**C8**, 87	85 : 15	87
9	Et/5,6-$(OMe)_2$	56	**C9**, 93	85 : 15	94
10	Et/6-Me	20	**C10**, 91	90 : 10	94
11	Et/7-F	8	**C11**, 91	85 : 15	85
12	Et/7-Cl	8	**C12**, 87	90 : 10	86
13	Et/7-CF_3	8	**C13**, 92	81 : 19	67
14	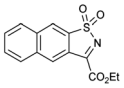	72	**C14**, 77	87 : 13	80

[a] Unless otherwise noted, all reactions were carried out with **L_3-PiMe$_2$Br**/Ni(OTf)$_2$ (1 : 1, 10 mol%), **A** (0.10 mmol), **B1** (0.20 mmol) and $LiNTf_2$ (30 mol%) in CH_2Cl_2 (2.5 mL) at room temperature under a N_2 atmosphere and 2 W LED (λ_{max} = 365 nm) for a certain time. [b] Isolated yield of **C**. [c] Determined by ^{1}H NMR analysis. [d] Determined by UPC^2 on a chiral stationary phase.

80 : 20–90 : 10 dr and 67–87% ee). Imine with fused naphthyl could also be transformed into the desired product **C14** but in 77% yield, 87 : 13 dr and 80% ee (Table 2, entry 14).

Next, the scope of 2-benzylbenzophenone derivatives was examined (Table 3). The 2-benzophenones **B** with electron-donating groups (2-Me, 4-OMe) on the Ar unit afforded the desired adducts (**C15–C16**) in lower yields (78–81%) and enantioselectivities (84 : 16–90 : 10 dr and 63–78% ee) than those containing electron-deficient aryl subunits (**C17–C20**, 85–99% yields, 74 : 26–89 : 11 dr and 92–95% ee). Nevertheless, the enantioselectivity dropped dramatically in the case of 4-CN and 2-thienyl substituted substrates (**B21** and **B22**), probably due to the interferential coordination between the CN group or thienyl of ketone substrates with a central metal ion. Moreover, electron-withdrawing and electron-donating substituents (R) were well tolerated. 5-Methyl substituted substrate **B23** gave relatively lower enantioselectivity than others, perhaps on account of the higher reactivity of photoenols that led to a strong background reaction. The steric hindrance of the R′ side-group has a pronounced effect on this transformation. The substrate bearing the *ortho*-fluorophenyl group was an exception to give the desired product (**C28**) smoothly (82% yield) with poor stereoselectivity (41 : 59 dr, 65%/55% ee). A broad array of benzophenones with electron-withdrawing and electron-donating substituents at the *meta*- and *para*-positions could

Table 3 Substrate scope of 2-benzylbenzophenone derivatives[a]

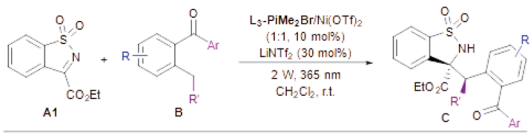

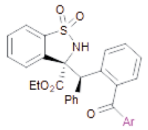

C15, Ar = 2-MeC_6H_4, 9.5 h, 81% yield, 90:10 dr, 63% ee
C16, Ar = 4-MeOC_6H_4, 8 h, 78% yield, 84:16 dr, 78% ee
C17, Ar = 3-FC_6H_4, 8 h, 99% yield, 79:21 dr, 93% ee
C18, Ar = 4-FC_6H_4, 8 h, 90% yield, 89:11 dr, 93% ee
C19, Ar = 4-ClC_6H_4, 8 h, 92% yield, 84:16 dr, 95% ee
C20, Ar = 4-$F_3CC_6H_4$, 10 h, 85% yield, 74:26 dr, 92% ee
C21, Ar = 4-CNC_6H_4, 28 h, 65% yield, 87:13 dr, 41% ee
C22, Ar = 2-thieny, 82 h, 42% yield, 75:25 dr, 73% ee

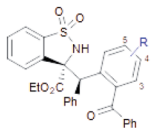

C23, R = 5-Me, 8 h, 86% yield, 88:12 dr, 77% ee
C24, R = 4-Me, 8 h, 98% yield, 87:13 dr, 91% ee
C25, R = 5-F, 8 h, 88% yield, 88:12 dr, 93% ee
C26, R = 4-Cl, 8 h, 99% yield, 94:6 dr, 95% ee
C27, R = 4-CF_3, 8 h, 94% yield, 89:11 dr, 88% ee

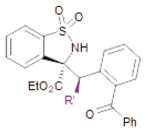

C28, R′ = 2-FC_6H_4, 10 h, 82% yield, 41:59 dr, 65%/55% ee
C29, R′ = 3-FC_6H_4, 17 h, 98% yield, 80:20 dr, 91% ee
C30, R′ = 3-MeC_6H_4, 9 h, 92% yield, 91:9 dr, 91% ee
C31, R′ = 3-ClC_6H_4, 9 h, 95% yield, 81:19 dr, 88% ee
C32, R′ = 3,4-$Cl_2C_6H_3$, 10.5 h, 96% yield, 78:22 dr, 85% ee
C33, R′ = 3,4-(OCH_2O)-C_6H_3, 35 h, 64% yield, 92:8 dr, 91% ee
C34, R′ = 4-PhC_6H_4, 12 h, 78% yield, 87:13 dr, 88% ee
C35, R′ = 4-FC_6H_4, 10 h, 94% yield, 79:21 dr, 88% ee
C36, R′ = 4-ClC_6H_4, 9.5 h, 96% yield, 90:10 dr, 94% ee
C37, R′ = 4-$F_3CC_6H_4$, 10 h, 91% yield, 78:22 dr, 87% ee
C38, R′ = 4-MeC_6H_4, 8 h, 96% yield, 89:11 dr, 89% ee
C39, R′ = 4-MeOC_6H_4, 24 h, 67% yield, 92:8 dr, 84% ee
C40, R′ = 3-furyl, 30 h, 64% yield, 96:4 dr, 90% ee
C41, R′ = 3-thienyl, 48 h, 92% yield, 92:8 dr, 88% ee
C42, R′ = Me, 8 h, 87% yield, 48:52 dr, 93%/83% ee
C43, R′ = H, 8 h, 54% yield, 61% ee

[a] Unless otherwise noted, all reactions were carried out with **L_3-PiMe$_2$Br**/Ni(OTf)$_2$ (1 : 1, 10 mol%), **A1** (0.10 mmol), **B** (0.20 mmol) and $LiNTf_2$ (30 mol%) in CH_2Cl_2 (2.5 mL) at room temperature under a N_2 atmosphere and 2 W LED (λ_{max} = 365 nm) for a certain time. The isolated yield of **C** is provided. The dr value was determined by ^{1}H NMR analysis and the ee value was determined by UPC^2 on a chiral stationary phase or chiral HPLC analysis.

be transformed to the corresponding products in good yields with moderate dr and high ee (**C29–C39**). To our delight, 3-furyl and 3-thienyl substituted substrates were also suitable under this catalytic system (**C40–C41**). However, low diastereoselectivity with maintained enantioselectivity was obtained when (2-ethylphenyl)(phenyl)methanone participated in (Me, **C42**), implying the high importance of an aryl substituent at the terminal of the photoenol intermediate to diastereocontrol. Furthermore, an obvious decrease in yield and the ee value of the desired Mannich product (**C43**) was obtained along with the formation of a *retro*-aza-vinylogous Michael product (18% yield) if phenyl(*o*-tolyl)methanone was employed in the reaction (see the ESI† for details).

Subsequently, we turned our attention to the scope of aryl/alkyl-type of ketones (Table 4). Under the modified reaction conditions (see the ESI† for details), photoexcitation of *ortho*-methyl acetophenone **B44** produced the photoenol followed by the Mannich reaction to provide the addition product smoothly, which was unstable and intended to undergo ring-closure for the construction of a tetracyclic skeleton (**D1**, 60% yield and

Table 4 Substrate scope of aryl/alkyl-type of ketones[a]

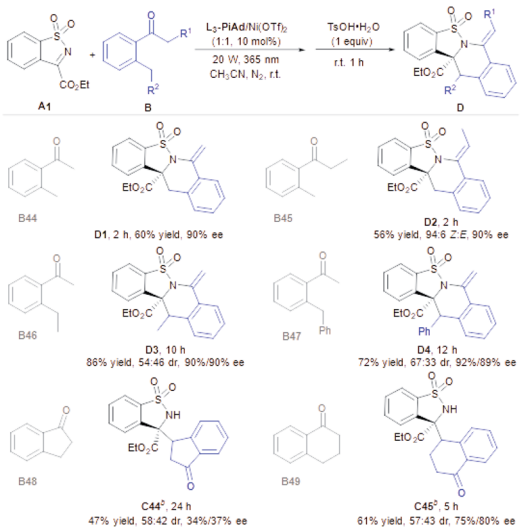

[a] Unless otherwise noted, all reactions were carried out with **L_3-PiAd**/$Ni(OTf)_2$ (1 : 1, 10 mol%), **A** (0.10 mmol) and **B** (0.20 mmol) in CH_3CN (1.0 mL) at room temperature under a N_2 atmosphere and 20 W LED (λ_{max} = 365 nm) for a certain time, and then $TsOH \cdot H_2O$ was added and stirred at room temperature for another 1 h under air. The isolated yield of **D** or **C** is provided. The dr value was determined by ^1H NMR analysis and the ee value was determined by UPC^2 on a chiral stationary phase or chiral HPLC analysis. [b] Without further transformation in the presence of $TsOH \cdot H_2O$.

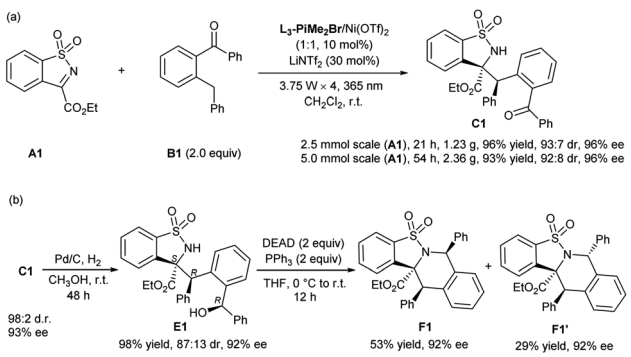

Scheme 2 Gram-scale synthesis and further transformations.

90% ee) by dealing with $TsOH \cdot H_2O$. This finding almost excluded the generally supposed cycloaddition pathway.[13] As such, *ortho*-methyl propiophenone (**B45**) provided the tetrahydroisoquinoline derivative **D2** in 56% yield with 90% ee. It was worth noting that the *Z* : *E* ratio of **D2** increased to 94 : 6 with the extension of time, which indicated that the β-H elimination step is reversible (see the ESI† for details). 2-Ethyl acetophenone **B46** and 2-benzyl acetophenone **B47** were also effective to generate the desired cyclization products **D3** and **D4** in good yields with excellent enantioselectivities (72–86% yields and 90–92% ee), but the diastereoselectivities (54 : 46–67 : 33 dr) were poor even though the intensity of the light source was lowered. Benzannulated carbocyclic ketones, such as 1-indanone and 1-tetralone, were acceptable substrates as well to form the photoenols and incorporated into *N*-sulfonyl cyclic ketimine to provide **C44** and **C45** smoothly (47–71% yields, 58 : 42–57 : 43 dr and 34–75% ee), but no ring-closure products were observed with $TsOH \cdot H_2O$.

To show the synthetic potential of the current protocol, the gram-scale synthesis of **C1** was conducted under slightly modified optimal conditions. Considering the difference in reaction vessels, four 3.75 W LEDs (λ_{max} = 365 nm) were used (see the ESI† for details). As shown in Scheme 2a, *N*-sulfonyl cyclic ketimine **A1** reacted with 2-benzylbenzophenone **B1** smoothly, providing **C1** (2.5 mmol scale, 1.23 g; 5 mmol scale, 2.36 g) with maintained yield, and diastereo- and enantioselectivity. Treatment of **C1** with Pd/C and H_2 afforded the reduction alcohol **E1** in nearly equivalent yield, 87 : 13 dr and 92%/82% ee (Scheme 2b), and the absolute configuration of the major enantiomer was determined to be (*S*,*R*,*R*) by X-ray crystallographic analysis.[16b] The intramolecular Mitsunobu reaction of **E1** proceeded well under the conventional reaction conditions,[17] and afforded the tetrahydroisoquinoline derivatives **F1** and **F1′** with maintained enantioselectivities. The absolute configuration of **F1′** was determined to be (*S*,*R*,*R*) by X-ray crystallographic analysis.[16c]

In order to gain insight into the mechanism of the PEM reaction, some control experiments were carried out. In the illumination experiments of the product (Table 5), **C1** could be recovered with basically maintained stereoselectivity under the standard conditions for 10 h (Table 5, entry 1). On changing the wavelength to 385 nm, the diastereoselectivity dropped sharply due to the fast epimerization (Table 5, entry 2), which explained the low diastereoselectivity of the PEM reaction under a 385 nm UV LED (Table 1, entry 11). In the absence of the **L_3-PiMe$_2$Br**/$Ni(OTf)_2$ complex, the stereoselectivity of **C1** was nearly unchanged (Table 5, entry 3). However, the diastereoselectivity

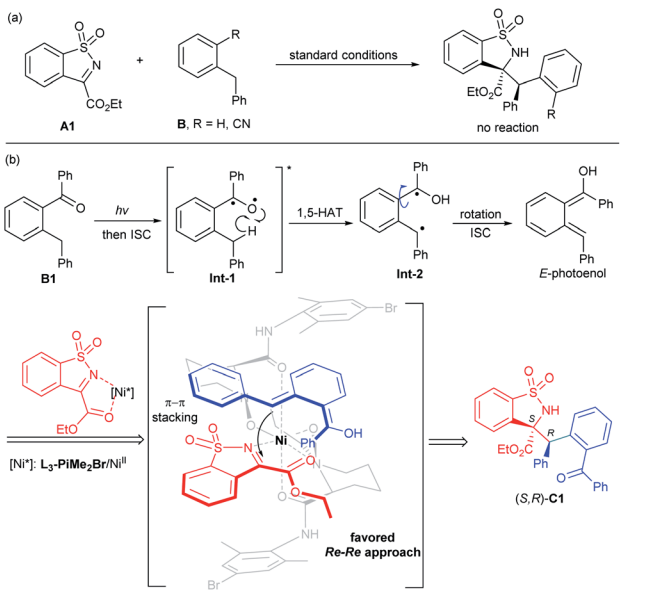

Scheme 3 Control experiments and the proposed reaction process of the asymmetric PEM reaction.

Table 5 The illumination experiment of **C1**[a]

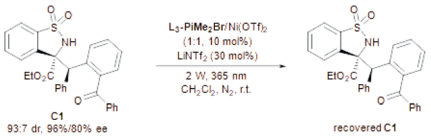

Entry	Variation from the standard conditions	Yield[b] (%)	dr[c]	ee[d] (%)
1	—	89	91 : 9	96/87
2	2 W, 385 nm	74	37 : 63	95/93
3	No **L_3-PiMe$_2$Br**/Ni(OTf)$_2$	83	92 : 8	96/82
4	No LiNTf$_2$	92	79 : 21	96/91
5	20 W, no LiNTf$_2$, 20 h	51	10 : 90	76/95
6	20 W, no catalyst, 20 h	52	11 : 89	78/95

[a] Unless otherwise noted, all reactions were carried out with **L_3-PiMe$_2$Br**/Ni(OTf)$_2$ (1 : 1, 10 mol%), **C1** (0.10 mmol) and LiNTf$_2$ (30 mol%) in CH_2Cl_2 (2.5 mL) at room temperature under a N_2 atmosphere and 2 W LED (λ_{max} = 365 nm) for 10 h. [b] Isolated yield of **C**. [c] Determined by ^{1}H NMR analysis. [d] Determined by UPC^2 on a chiral stationary phase.

sharply decreased without LiNTf$_2$ (Table 5, entry 4). These results suggested that the additive LiNTf$_2$ may not only provide counterions for the chiral catalyst, but also coordinate with the carbonyl group of **C1** to impede the epimerization. Interestingly, by increasing the illumination intensity to 20 W and extending the illumination time to 20 h without LiNTf$_2$, the diastereoselectivity could be reversed through the second photoenolization of **C1** albeit with partial decomposition (Table 5, entry 5), and the simple illumination with none of the catalysts gave a similar result (Table 5, entry 6), which provided a possibility for diastereodivergent synthesis.[18] Additionally, no reaction occurred when replacing the benzoyl group with a nitrile group or hydrogen atom, but a self-coupling product of the imine was observed. It excluded the direct intermolecular hydrogen atom transfer process of excited imine[19] with 2-benzyl benzophenone (Scheme 3a).

Based on the experimental results, the absolute configuration of the product **C1** and our previous studies,[20] a plausible transition state model was proposed (Scheme 3b). Under UV irradiation, the biradical **Int-2** was obtained through 1,5-hydrogen atom transfer (HAT) of the triplet excited 2-benzylbenzophenone **Int-1**. Rotation of this biradical species and subsequent intersystem crossing (ISC) led to the reactive intermediate *E*-photoenol. According to the above experimental results, we conjectured that a π–π interaction between the aryl group at the benzyl position of the photoenol and the aryl group of *N*-sulfonyl cyclic ketimine exists. Meanwhile, the *N*,*N*′-dioxide/Ni^{II} complex activated the imine **A1** in a bidentate coordination manner and the *Si* face of imine was shielded by the amide unit of the ligand. Thus, the *Re*–*Re* nucleophilic addition generated the Mannich product (*S*,*R*)-**C1**.

Conclusions

In summary, we have developed the first Lewis acid-catalyzed asymmetric PEM reaction. The combination of a chiral *N*,*N*′-dioxide/Ni^{II} complex catalyst and LiNTf$_2$ could effectively suppress the background reaction and the epimerization of the products, offering a broad array of optically active α-amino acid ester derivatives with excellent stereoselectivities, and a reversal of diastereoselectivity was also achieved. The tetracyclic ring-closure products could be further yielded in one pot. In addition, the results of control experiments ruled out the general hetero-Diels–Alder/ring-opening sequence and the intermolecular direct HAT process. A plausible transition state model involving photo-mediated enol was also proposed to explain the origin of stereoselective control.

Data availability

Further details of experimental procedure, ^{1}H, ^{13}C{^{1}H} and ^{19}F{^{1}H} NMR, HPLC spectra, CD spectra and X-ray crystallographic data are available in the ESI.†

Author contributions

L. K. Y. performed the experiments. W.-Y. L. repeated the data. L. Z. H. and T. Y. Z. participated in the synthesis of substrates and ligands. X. M. F., X. H. L. and W. D. C. supervised the project. X. H. L., W. D. C. and L. K. Y. co-wrote the manuscript.

Conflicts of interest

There are no conflicts to declare.

Acknowledgements

We appreciate the National Natural Science Foundation of China (No. 22071160 and 22188101) and the Science & Technology Department of Sichuan Province (No. 2021YJ0562) for financial support. We are grateful to Dr Yuqiao Zhou from the College of Chemistry, Sichuan University for the X-ray single crystal diffraction analysis.

Notes and references

1 For leading reviews, see: (*a*) J. M. R. Narayanam and C. R. J. Stephenson, *Chem. Soc. Rev.*, 2011, **40**, 102–113; (*b*) J. Xuan and W.-J. Xiao, *Angew. Chem., Int. Ed.*, 2012, **51**, 6828–6838; (*c*) C. K. Prier, D. A. Rankic and D. W. C. MacMillan, *Chem. Rev.*, 2013, **113**, 5322–5363; (*d*) Y. Xi, H. Yi and A. Lei, *Org. Biomol. Chem.*, 2013, **11**, 2387–2403; (*e*) J. Xuan, L.-Q. Lu, J.-R. Chen and W.-J. Xiao, *Eur. J. Org. Chem.*, 2013, 6755–6770; (*f*) D. A. Nicewicz and T. M. Nguyen, *ACS Catal.*, 2014, **4**, 355–360; (*g*) D. M. Schultz and T. P. Yoon, *Science*, 2014, **343**, 1239176; (*h*) R. A. Angnes, Z. Li, C. R. D. Correia and G. B. Hammond, *Org. Biomol. Chem.*, 2015, **13**, 9152–9167; (*i*) R. Brimioulle, D. Lenhart, M. M. Maturi and T. Bach, *Angew. Chem., Int. Ed.*, 2015, **54**, 3872–3890; (*j*) J.-R. Chen, X.-Q. Hu, L.-Q. Lu and W.-J. Xiao, *Chem. Soc. Rev.*, 2016, **45**, 2044–2056; (*k*) J.-R. Chen, X.-Q. Hu, L.-Q. Lu and W.-J. Xiao, *Acc. Chem. Res.*, 2016, **49**, 1911–1923; (*l*) D. Ravelli, S. Protti and M. Fagnoni, *Chem. Rev.*, 2016, **116**, 9850–9913; (*m*) J. Twilton, C. Le, P. Zhang, M. H. Shaw, R. W. Evans and D. W. C. MacMillan, *Nat. Rev. Chem.*, 2017, **1**, 52; (*n*) D. Wang, L. Zhang and S. Luo, *Acta Chim. Sin.*, 2017, **75**, 22–33; (*o*) M. Silvi and P. Melchiorre, *Nature*, 2018, **554**, 41–49; (*p*) B.-G. Cai, J. Xuan and W.-J. Xiao, *Sci. Bull.*, 2019, **64**, 337–350; (*q*) Q.-Q. Zhou, Y.-Q. Zou, L.-Q. Lu and W.-J. Xiao, *Angew. Chem., Int. Ed.*, 2019, **58**, 1586–1604; (*r*) W.-M. Cheng and R. Shang, *ACS Catal.*, 2020, **10**, 9170–9196; (*s*) H. Cao, X. Tang, H. Tang, Y. Yuan and J. Wu, *Chem Catalysis*, 2021, **1**, 523–598; (*t*) T. Yasukawa and S. Kobayashi, *ACS Cent. Sci.*, 2021, **7**, 1099–1101; (*u*) X.-Y. Yu, J.-R. Chen and W.-J. Xiao, *Chem. Rev.*, 2021, **121**, 506–561; (*v*) L. Capaldo, D. Ravelli and M. Fagnoni, *Chem. Rev.*, 2022, **122**, 1875–1924; (*w*) A. Y. Chan, I. B. Perry, N. B. Bissonnette, B. F. Buksh, G. A. Edwards, L. I. Frye, O. L. Garry, M. N. Lavagnino, B. X. Li, Y. Liang, E. Mao, A. Millet, J. V. Oakley, N. L. Reed, H. A. Sakai, C. P. Seath and D. W. C. MacMillan, *Chem. Rev.*, 2022, **122**, 1485–1542; (*x*) M. J. Genzink, J. B. Kidd, W. B. Swords and T. P. Yoon, *Chem. Rev.*, 2022, **122**, 1654–1716; (*y*) J. Großkopf, T. Kratz, T. Rigotti and T. Bach, *Chem. Rev.*, 2022, **122**, 1626–1653; (*z*) N. Holmberg-Douglas and D. A. Nicewicz, *Chem. Rev.*, 2022, **122**, 1925–2016; (*aa*) P. Melchiorre, *Chem. Rev.*, 2022, **122**, 1483–1484.

2 For the reviews, see: (*a*) T. Bach and J. P. Hehn, *Angew. Chem., Int. Ed.*, 2011, **50**, 1000–1045; (*b*) S. Gao and Y. Qiu, *Sci. China: Chem.*, 2016, **59**, 1093–1108; (*c*) M. D. Kärkäs, J. A. Porco and C. R. J. Stephenson, *Chem. Rev.*, 2016, **116**, 9683–9747; (*d*) T. P. Nicholls, D. Leonori and A. C. Bissember, *Nat. Prod. Rep.*, 2016, **33**, 1248–1254; (*e*) M. K. Bogdos, E. Pinard and J. A. Murphy, *Beilstein J. Org. Chem.*, 2018, **14**, 2035–2064; (*f*) B. Yang and S. Gao, *Chem. Soc. Rev.*, 2018, **47**, 7926–7953; (*g*) Y. Wei, Q.-Q. Zhou, F. Tan, L.-Q. Lu and W.-J. Xiao, *Synthesis*, 2019, **51**, 3021–3054; (*h*) C. M. Holden and P. Melchiorre, in *Photochemistry*, The Royal Society of Chemistry, 2020, vol. 47, pp. 344–378; (*i*) J. B. Mateus-Ruiz and A. Cordero-Vargas, *Synthesis*, 2020, **52**, 3111–3128.

3 For selected reviews and examples of photoreactivity of aromatic aldehydes and ketones, see: (*a*) R. G. W. Norrish and C. H. Bamford, *Nature*, 1937, **140**, 195–196; (*b*) N. C. Yang and D.-D. H. Yang, *J. Am. Chem. Soc.*, 1958, **80**, 2913–2914; (*c*) A. Dalal, R. Khanna, D. Kumar, P. Jindal, A. Chaudhary and R. C. Kamboj, *Curr. Org. Chem.*, 2015, **19**, 2156–2195; (*d*) C. Chen, *Org. Biomol. Chem.*, 2016, **14**, 8641–8647; (*e*) M. Oelgemöller and N. Hoffmann, *Org. Biomol. Chem.*, 2016, **14**, 7392–7442; (*f*) M. D'Auria, *Photochem. Photobiol. Sci.*, 2019, **18**, 2297–2362; (*g*) J. A. Dantas, J. T. M. Correia, M. W. Paixão and A. G. Corrêa, *ChemPhotoChem*, 2019, **3**, 506–520; (*h*) W. Zhang, Y. Li and S. Luo, *J. Photochem. Photobiol., A*, 2020, **396**, 112553; (*i*) J. Jurczyk, M. C. Lux, D. Adpressa, S. F. Kim, Y.-h. Lam, C. S. Yeung and R. Sarpong, *Science*, 2021, **373**, 1004–1012; (*j*) J. Mateos, S. Cuadros, A. Vega-Peñaloza and L. Dell'Amico, *Synlett*, 2022, **33**, 116–128.

4 (*a*) N. C. Yang and C. Rivas, *J. Am. Chem. Soc.*, 1961, **83**, 2213; (*b*) P. G. Sammes, *Tetrahedron*, 1976, **32**, 405–422; (*c*) J. L. Segura and N. Martín, *Chem. Rev.*, 1999, **99**, 3199–3246; (*d*) A. Mavroskoufis, K. Rajes, P. Golz, A. Agrawal, V. Ruß, J. P. Götze and M. N. Hopkinson, *Angew. Chem., Int. Ed.*, 2020, **59**, 3190–3194.

5 For selected reviews and examples of reactions involving photoenols, see: (*a*) J. L. Charlton and M. M. Alauddin, *Tetrahedron*, 1987, **43**, 2873–2889; (*b*) J. L. Charlton and K. Koh, *J. Org. Chem.*, 1992, **57**, 1514–1516; (*c*) R. Connors and T. Durst, *Tetrahedron Lett.*, 1992, **33**, 7277–7280; (*d*) G. A. Kraus and Y. Wu, *J. Org. Chem.*, 1992, **57**, 2922–2925; (*e*) K. C. Nicolaou, D. Gray and J. Tae, *Angew. Chem., Int. Ed.*, 2001, **40**, 3675–3678; (*f*) K. C. Nicolaou, D. Gray and J. Tae, *Angew. Chem., Int. Ed.*, 2001, **40**, 3679–3683; (*g*) K. Takaki, T. Fujii, H. Yonemitsu, M. Fujiwara, K. Komeyama and H. Yoshida, *Tetrahedron Lett.*, 2012, **53**, 3974–3976; (*h*) Y. Masuda, N. Ishida and M. Murakami, *J. Am. Chem. Soc.*, 2015, **137**, 14063–14066; (*i*) T. Ide, S. Masuda, Y. Kawato, H. Egami and Y. Hamashima, *Org. Lett.*, 2017, **19**, 4452–4455; (*j*) N. Ishida, T. Yano, T. Yuhki and M. Murakami, *Chem.–Asian J.*, 2017, **12**, 1905–1908; (*k*) S. Cuadros and P. Melchiorre, *Eur. J. Org. Chem.*, 2018, 2884–2891; (*l*) J. Mateos, A. Cherubini-Celli, T. Carofiglio, M. Bonchio, N. Marino, X. Companyó and L. Dell'Amico, *Chem. Commun.*, 2018, **54**, 6820–6823; (*m*) Y. Masuda, N. Ishida and M. Murakami, *Chem.–Asian J.*, 2019, **14**, 403–406; (*n*) J. Mateos, F. Rigodanza, A. Vega-Peñaloza, A. Sartorel, M. Natali, T. Bortolato, G. Pelosi, X. Companyó, M. Bonchio and L. Dell'Amico, *Angew. Chem., Int. Ed.*, 2020, **59**, 1302–1312; (*o*) Y. Zhang, R. Jin, W. Kang and H. Guo, *Org. Lett.*, 2020, **22**, 5502–5505; (*p*) Y. Zhang, R. Jin, G. Pan and H. Guo, *Chem. Commun.*, 2020, **56**, 11621–11624; (*q*) J. Y. J. Wang, M. T. Blyth, M. S. Sherburn and M. L. Coote, *J. Am. Chem. Soc.*, 2022, **144**, 1023–1033; (*r*) Z.-L. Wang, L. Tang, W.-M. Zeng, Y.-H. He and Z. Guan, *Tetrahedron Lett.*, 2022, **95**, 153725.

6 B. Grosch, C. N. Orlebar, E. Herdtweck, W. Massa and T. Bach, *Angew. Chem., Int. Ed.*, 2003, **42**, 3693–3696.
7 K. C. Nicolaou, D. L. F. Gray and J. Tae, *J. Am. Chem. Soc.*, 2004, **126**, 613–627.
8 L. Dell'Amico, A. Vega-Peñaloza, S. Cuadros and P. Melchiorre, *Angew. Chem., Int. Ed.*, 2016, **55**, 3313–3317.
9 (*a*) B. Yang, K. Lin, Y. Shi and S. Gao, *Nat. Commun.*, 2017, **8**, 622; (*b*) D. Xue, M. Xu, C. Zheng, B. Yang, M. Hou, H. He and S. Gao, *Chin. J. Chem.*, 2019, **37**, 135–139; (*c*) D. Jiang, K. Xin, B. Yang, Y. Chen, Q. Zhang, H. He and S. Gao, *CCS Chem.*, 2020, **2**, 800–812; (*d*) M. Hou, M. Xu, B. Yang, H. He and S. Gao, *Chem. Sci.*, 2021, **12**, 7575–7582; (*e*) M. Hou, M. Xu, B. Yang, H. He and S. Gao, *Org. Lett.*, 2021, **23**, 7487–7491; (*f*) X.-L. Lu, Y. Qiu, B. Yang, H. He and S. Gao, *Chem. Sci.*, 2021, **12**, 4747–4752; (*g*) X.-L. Lu, B. Yang, H. He and S. Gao, *Org. Chem. Front.*, 2021, **8**, 1143–1148; (*h*) M. Xu, M. Hou, H. He and S. Gao, *Angew. Chem., Int. Ed.*, 2021, **60**, 16655–16660; (*i*) B. Yang, G. Wen, Q. Zhang, M. Hou, H. He and S. Gao, *J. Am. Chem. Soc.*, 2021, **143**, 6370–6375; (*j*) Q. Zhang, H. He and S. Gao, *Chem. Commun.*, 2022, **58**, 4239–4242.
10 (*a*) L. Dell'Amico, V. M. Fernández-Alvarez, F. Maseras and P. Melchiorre, *Angew. Chem., Int. Ed.*, 2017, **56**, 3304–3308; (*b*) X. Yuan, S. Dong, Z. Liu, G. Wu, C. Zou and J. Ye, *Org. Lett.*, 2017, **19**, 2322–2325.
11 (*a*) S. Cuadros, L. Dell'Amico and P. Melchiorre, *Angew. Chem., Int. Ed.*, 2017, **56**, 11875–11879; (*b*) S. Cao, J. Li, T. Yan, J. Han and Z. He, *Org. Chem. Front.*, 2022, **9**, 643–648.
12 S. Paria, E. Carletti, M. Marcon, A. Cherubini-Celli, A. Mazzanti, M. Rancan, L. Dell'Amico, M. Bonchio and X. Companyó, *J. Org. Chem.*, 2020, **85**, 4463–4474.
13 H. B. Hepburn, G. Magagnano and P. Melchiorre, *Synthesis*, 2017, **49**, 76–86.
14 For reviews and selected examples on chiral *N*,*N*′-dioxides, see: (*a*) X. H. Liu, L. L. Lin and X. M. Feng, *Acc. Chem. Res.*, 2011, **44**, 574–587; (*b*) X. H. Liu, L. L. Lin and X. M. Feng, *Org. Chem. Front.*, 2014, **1**, 298–302; (*c*) X. H. Liu, H. F. Zheng, Y. Xia, L. L. Lin and X. M. Feng, *Acc. Chem. Res.*, 2017, **50**, 2621–2631; (*d*) X. H. Liu, S. X. Dong, L. L. Lin and X. M. Feng, *Chin. J. Chem.*, 2018, **36**, 791–797; (*e*) T. F. Kang, W. D. Cao, L. Z. Hou, Q. Tang, S. J. Zou, X. H. Liu and X. M. Feng, *Angew. Chem., Int. Ed.*, 2019, **58**, 2464–2468; (*f*) Z. Wang, X. H. Liu and X. M. Feng, *Aldrichimica Acta*, 2020, **53**, 3–10; (*g*) M. Y. Wang and W. Li, *Chin. J. Chem.*, 2021, **39**, 969–984; (*h*) X. B. Lin, Z. Tan, W. K. Yang, W. Yang, X. H. Liu and X. M. Feng, *CCS Chem.*, 2021, **3**, 1423–1433; (*i*) G. H. Pan, C. L. He, M. Chen, Q. Xiong, W. D. Cao and X. M. Feng, *CCS Chem.*, 2021, **3**, 2012–2020. For examples in photocatalysis:(*j*) H. Yu, S. X. Dong, Q. Yao, L. Chen, D. Zhang, X. H. Liu and X. M. Feng, *Chem.–Eur. J.*, 2018, **24**, 19361–19367; (*k*) C.-X. Ye, Y. Y. Melcamu, H.-H. Li, J.-T. Cheng, T.-T. Zhang, Y.-P. Ruan, X. Zheng, X. Lu and P.-Q. Huang, *Nat. Commun.*, 2018, **9**, 410; (*l*) D. Zhang, Z. S. Su, Q. W. He, Z. K. Wu, Y. Q. Zhou, C. J. Pan, X. H. Liu and X. M. Feng, *J. Am. Chem. Soc.*, 2020, **142**, 15975–15985; (*m*) H. Yu, T. Y. Zhan, Y. Q. Zhou, L. Chen, X. H. Liu and X. M. Feng, *ACS Catal.*, 2022, **12**, 5136–5144; (*n*) Z. D. Tan, S. B. Zhu, Y. B. Liu and X. M. Feng, *Angew. Chem., Int. Ed.*, 2022, e202203374.
15 Lithium salts with different counterions (LiCl, $LiBF_4$, and LiOTf) and $NaNTf_2$ were examined as well. The results showed that NTf_2^- plays an important role in enhancement of stereoselectivity (see the ESI† for details).
16 (*a*) CCDC 2081680 (**C1**); †; (*b*) CCDC 2130299 (**E1**); †; (*c*) CCDC 2171982 (**F1′**).†
17 (*a*) M. Oyo and Y. Masaaki, *Bull. Chem. Soc. Jpn.*, 1967, **40**, 2380–2382; (*b*) M. Oyo, Y. Masaaki and M. Teruaki, *Bull. Chem. Soc. Jpn.*, 1967, **40**, 935–939; (*c*) T. Fukuyama, C.-K. Jow and M. Cheung, *Tetrahedron Lett.*, 1995, **36**, 6373–6374; (*d*) N. García-Delgado, A. Riera and X. Verdaguer, *Org. Lett.*, 2007, **9**, 635–638.
18 For selected reviews of diastereodivergent synthesis, see: (*a*) M. Bihani and J. C.-G. Zhao, *Adv. Synth. Catal.*, 2017, **359**, 534–575; (*b*) S. Krautwald and E. M. Carreira, *J. Am. Chem. Soc.*, 2017, **139**, 5627–5639; (*c*) L. L. Lin and X. M. Feng, *Chem.–Eur. J.*, 2017, **23**, 6464–6482; (*d*) G. Zhan, W. Du and Y.-C. Chen, *Chem. Soc. Rev.*, 2017, **46**, 1675–1692; (*e*) I. P. Beletskaya, C. Nájera and M. Yus, *Chem. Rev.*, 2018, **118**, 5080–5200.
19 For reviews of photoreactivity of imines, see: (*a*) A. Padwa, *Chem. Rev.*, 1977, **77**, 37–68; (*b*) A. C. Pratt, *Chem. Soc. Rev.*, 1977, **6**, 63–81; (*c*) A. D. Richardson, M. R. Becker and C. S. Schindler, *Chem. Sci.*, 2020, **11**, 7553–7561; (*d*) D. Uraguchi, Y. Tsuchiya, T. Ohtani, T. Enomoto, S. Masaoka, D. Yokogawa and T. Ooi, *Angew. Chem., Int. Ed.*, 2020, **59**, 3665–3670; (*e*) S. K. Kandappa, L. K. Valloli, S. Ahuja, J. Parthiban and J. Sivaguru, *Chem. Soc. Rev.*, 2021, **50**, 1617–1641.
20 L. Z. Hou, T. F. Kang, L. K. Yang, W. D. Cao and X. M. Feng, *Org. Lett.*, 2020, **22**, 1390–1395.